Available online at www.sciencedirect.com

SCIENCE DIRECT®

Continental Shelf Research 26 (2006) 401–421

CONTINENTAL SHELF RESEARCH

www.elsevier.com/locate/csr

Cross-shore velocity shear, eddies and heterogeneity in water column properties over fringing coral reefs: West Maui, Hawaii

C.D. Storlazzi[a,*], M.A. McManus[b], J.B. Logan[a], B.E. McLaughlin[b]

[a] US Geological Survey, Pacific Science Center, Santa Cruz, CA 95064, USA

[b] Oceanography Department, University of Hawaii at Manoa, Honolulu, HI 96822, USA

Received 2 December 2004; received in revised form 21 September 2005; accepted 15 December 2005
Available online 21 February 2006

Abstract

A multi-day hydrographic survey cruise was conducted to acquire spatially extensive, but temporally limited, high-resolution, three-dimensional measurements of currents, temperature, salinity and turbidity off West Maui in the summer of 2003 to better understand coastal dynamics along a complex island shoreline with coral reefs. These data complement long-term, high-resolution tide, wave, current, temperature, salinity and turbidity measurements made at a number of fixed locations in the study area starting in 2001. Analyses of these hydrographic data, in conjunction with numerous field observations, evoke the following conceptual model of water and turbidity flux along West Maui. Wave- and wind-driven flows appear to be the primary control on flow over shallower portions of the reefs while tidal and subtidal currents dominate flow over the outer portions of the reefs and insular shelf. When the direction of these flows counter one another, which is quite common, they cause a zone of cross-shore horizontal shear and often form a front, with turbid, lower-salinity water inshore of the front and clear, higher-salinity water offshore of the front. It is not clear whether these zones of high shear and fronts are the cause or the result of the location of the fore reef, but they appear to be correlated alongshore over relatively large horizontal distances (orders of kilometers). When two flows converge or when a single flow is bathymetrically steered, eddies can be generated that, in the absence of large ocean surface waves, tend to accumulate material. Areas of higher turbidity and lower salinity tend to correlate with regions of poor coral health or the absence of well-developed reefs, suggesting that the oceanographic processes that concentrate and/or transport nutrients, contaminants, low-salinity water or suspended sediment might strongly influence coral reef ecosystem health and sustainability.
Published by Elsevier Ltd.

Keywords: Currents; Turbidity; Temperature; Salinity; Coral reefs; Shear; Eddies; Fronts

1. Introduction

Coral reefs typically grow in relatively clear, oligotrophic waters. Sewage injection, terrestrial runoff and groundwater percolation through the shoreface can introduce nutrients to the coastal zone (Coles and Ruddy, 1995; McKenna et al., 2001; Umezawa et al., 2002; Garrison et al., 2003).

*Corresponding author. Tel.: +1 831 427 4721; fax: +1 831 427 4748.

E-mail addresses: cstorlazzi@usgs.gov (C.D. Storlazzi), mamc@hawaii.edu (M.A. McManus), jlogan@usgs.gov (J.B. Logan), bem@soest.hawaii.edu (B.E. McLaughlin).

0278-4343/$ - see front matter Published by Elsevier Ltd.
doi:10.1016/j.csr.2005.12.006

These processes can modify coral-zooxanthellae population dynamics (Heikoop et al., 2000; Harrison and Ward, 2001), and increase macroalgal growth and subsequently produce overgrowth and death of corals (Szmant, 2002). Land use practices such as overgrazing and coastal development can increase the supply of terrestrial sediment to the nearshore. Lower than normal salinities due to freshwater discharge from streams or submarine groundwater discharge have been shown to reduce coral growth rates (Guzman and Tudhope, 1998), or at very low levels, kill corals (Jokiel et al., 1993). Fine-grained terrestrial sediment can smother corals and increase turbidity, which in turn, decreases light available for photosynthesis and can create physiological stress or even coral mortality (Acevedo et al., 1989; Fortes, 2000; Rogers, 1990; Buddemeir and Hopley, 1988). Toxic substances and heavy metals often adhere to fine-grained sediment, which become their transport mechanism into the nearshore reef ecosystem (Dickson et al., 1987; Saouter et al., 1993; Bastidas et al., 1999; Gee and Bruland, 2002).

West Maui, Hawaii, USA is characterized by a series of fringing reefs separated by sandy beaches and shorefaces. Over the past two decades, a number of factors have affected the quality of the nearshore waters off West Maui. Coastal development and agriculture has increased runoff and the supply of sediment to West Maui's coastal waters while terrestrial wastewater injection has increased the volume of nutrients percolating out of the shoreface via submarine groundwater discharge (Soicher and Peterson, 1996; West Maui Watershed Management Project, 1996; Dollar and Andrews, 1997). Using field data and a numerical groundwater model, Soicher and Peterson (1996) found that while groundwater sources provide a gradual, steady supply of nutrients to the coastal waters, ephemeral stream flow (generally during the winter months) at discrete locations discharges high levels of nitrogen, phosphorus and fine-grained terrestrial sediment into the nearshore region.

While a number of investigations have focused on wave-, wind- or tidally driven flow and transport along or across a specific reef (e.g. Roberts et al., 1977, 1980; Kraines et al., 1998; Lugo-Fernandez et al., 1998; Tartinville and Rancher, 2000; Storlazzi et al., 2004a), there have been limited investigations, however, of these physical processes on and between fringing reefs along an irregular volcanic island's shoreline. The goal of this study is to understand the spatial variability in flow patterns, water column properties and the processes governing the transport of larvae, fine-grained sediment, nutrient, contaminant and other particulate matter along a complex inner shelf with coral reefs. The observations described here, in conjunction with data from long-term, fixed oceanographic packages (Storlazzi and Jaffe, 2003; Storlazzi et al., 2003, 2004b), elucidate the complex interactions between the wind, waves, tides, and lower-frequency currents that drive hydrographic variability off West Maui. We hypothesize that these processes influence the development and present health of the reefs in the study area.

2. Study area

2.1. Geology

The island of Maui is located at 20.8°N, 156.5°W in the North-central Pacific between the islands of Molokai, Lanai and Hawaii ('the Big Island') in the Hawaiian Archipelago (Fig. 1). The island comprises two large basaltic shield volcanoes that formed in the last 2 million years (Clague and Dalrymple, 1989) that are separated by a flat isthmus. West Maui is roughly 30 km long in the north–south direction and on average 20 km wide in the east–west direction. Land use in the study area was historically dominated by pineapple and sugarcane cultivation; more recently, however, urbanization and development along the shoreline have increased substantially (M&E Pacific, 1991).

The shoreline in the study area is characterized by low basaltic seacliffs and carbonate sand beaches. The geomorphology of the inner shelf (<40 m depth) off West Maui in the Pailolo and Auau Channels between the islands of Maui, Lanai and Molokai is highly variable and includes boulders, small patches of sand, extensive sand fields and a number of patch and small fringing coral reefs with various exposures (Fig. 2a) as discussed by Gibbs et al. (2005). In areas exposed to large waves there is only a thin veneer of coral overlying a basaltic substrate, while in more protected areas live corals are growing on top of a relict reef structure. Reefs extend from the shoreline out to 1 km offshore in water depths of 30 m; the majority of the reefs are situated in water depths between 3 and 20 m. Coral coverage is very discontinuous in the study area, varying between 0% and 80% (Jokiel et al., 2001) even though there is adequate hard substrate

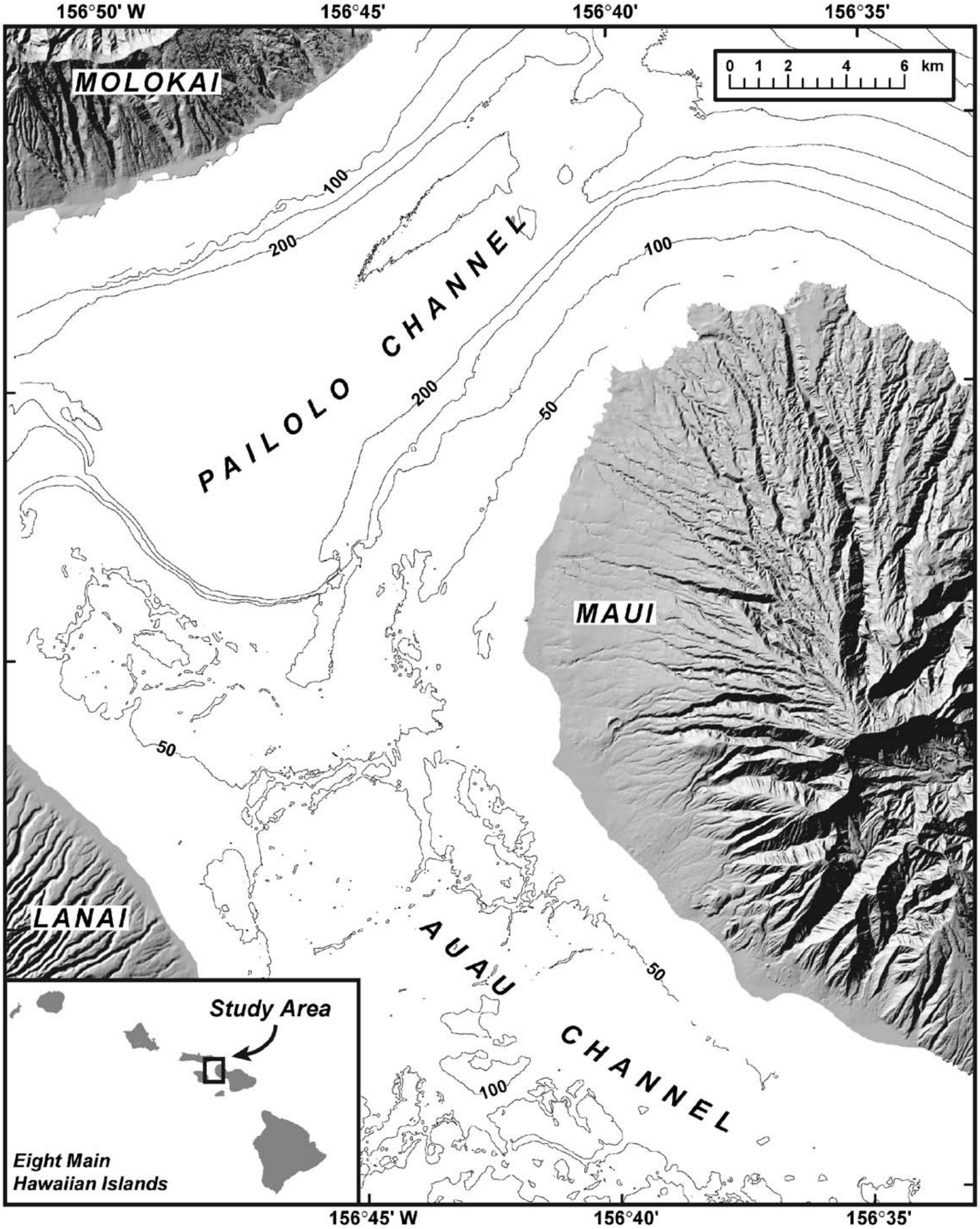

Fig. 1. Map of the study area location in relation to the adjacent main Hawaiian Islands. The study area is exposed to high wave energy gradients, with the northern and southern ends of the study area being impacted by the Northeast Trade wind waves and the Southern Ocean summer swell, respectively. The central portion of the study area, however, is in the lee of Molokai and the headland at Mala Wharf and thus receives very low wave energy.

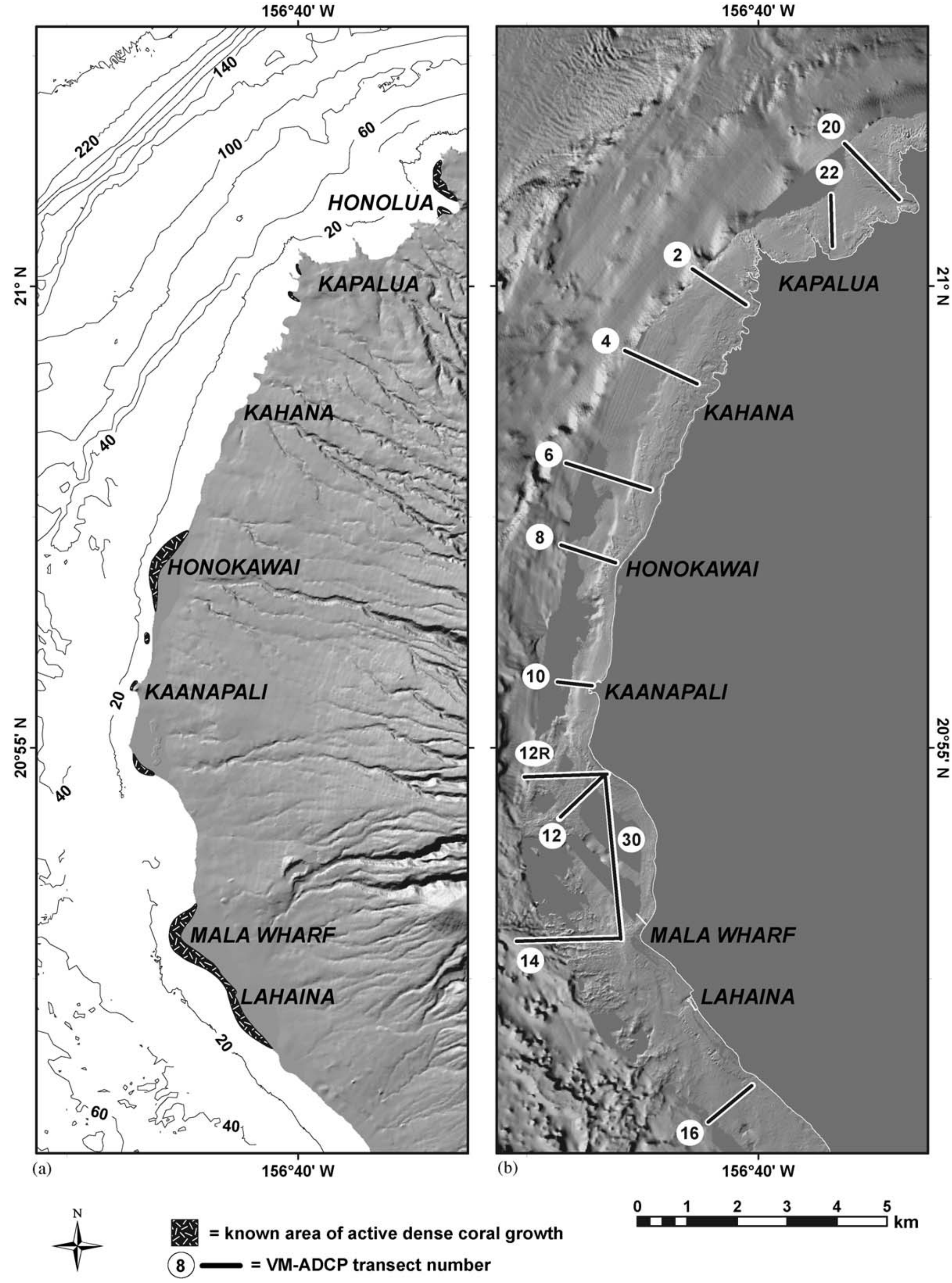
156°40' W
140
220
100
60
20
HONOLUA
KAPALUA
21° N
KAHANA
40
HONOKAWAI
KAANAPALI
20
20°55' N
40
MALA WHARF
LAHAINA
20
60
40
(a)
156°40' W
20
22
2
4
6
8
10
12R
12
30
14
16
(b)
0 1 2 3 4 5 km
N
= known area of active dense coral growth
8 = VM-ADCP transect number

available for new coral recruitment and active reef development (Gibbs et al., 2005).

2.2. Oceanography and meteorology

Until recently, the only studies investigating currents off West Maui looked at large-scale (order of 10's of km) flow through the channels between the islands of Lanai, Molokai and Maui (Flament and Lumpkin, 1996; Sun, 1996). Using satellite data and a numerical model, Sun (1996) observed long-term mean flow through the channels driven by differences in sea surface height across the island chain. Flament and Lumpkin (1996) deployed the first oceanographic mooring in the study area that was outfitted with current meters. These current meters were located roughly 25 and 210 m below the surface in the Pailolo Channel (water depth ~240 m), and were deployed for 19 months. They noted that the flow in the upper water column was primarily oriented east–west at 0–1.0 m/s (mean-0.04 m/s) while the flow closer to the bed was oriented southwest–northeast, roughly parallel to the isobaths, at 0–0.5 m/s (mean = 0.04 m/s). Flament and Lumpkin (1996) also calculated that the majority of the current's energy was in the diurnal and semi-diurnal tidal frequencies.

More recent studies by Storlazzi and Jaffe (2003), Storlazzi et al. (2003) and Storlazzi et al. (2004b) made measurements on the inner (<30 m) shelf, observing that the tidal wave propagated from south to north in the study area. Similar to the findings of Flament and Lumpkin (1996), they observed that flow over the deeper portion of the fore reef was dominated by diurnal and semi-diurnal tidal currents, and to a lesser extent, lower frequency motions likely driven by wind-driven differences in sea level across the island chain, as modeled by Merrifield et al. (2002). Over the reef flat, however, flows were primarily wind- and wave-driven, and they were often oriented at an angle (>90°) to the flows concurrently measured out over the fore reef.

The wave climate off west Maui is dominated by three end-members: North Pacific swell, Northeast Trade wind waves and Southern Ocean swell (Moberly and Chaimberlin, 1964). The North Pacific swell is generated by strong winter storms as they track from west to east across the North Pacific typically between November and March, generating significant wave heights (H_s) generally between 3 and 8 m and dominant periods (T_d) on the order of 10–20 s. The Northeast Trade wind waves occur throughout the year but are largest from April through November when the Trade winds are the strongest (typically 10–20 m/s; Ogston et al., 2004); these waves have H_s typically between 1 and 4 m and T_d on the order of 5–8 s. The Southern swell is generated by storms in the Southern Ocean during the Southern Hemisphere winter and while typical H_s are small (~1–2 m), these waves have long periods (T_d~14–25 s). Observations by Storlazzi and Jaffe (2003), Storlazzi et al. (2003) and Storlazzi et al. (2004b) noted strong gradients in wave energy off west Maui, with greater wave heights off northwest and southwest Maui and the lowest wave heights off the central part of west Maui.

Precipitation patterns on West Maui during the summer result primarily from orographic uplift of air masses driven by the Northeast Trade winds. The Northeast Trade winds strike the northeast side of West Maui, are steered around the West Maui volcanic cone and most often approach the shoreline obliquely from the north in the study area. Due to orographic effects associated with the high (>1400 m) West Maui shield volcano, most of the precipitation (100–400 cm/year) falls on the northern face of the volcano while the south and southwest sides of the volcano receive less than 40 cm/year on average (Fletcher et al., 2002). This causes a north–south gradient in both stream flow and terrestrial sediment discharge into the study area, with greater freshwater and sediment discharge in the northern portion of the study area between Honolua and Kahana than the southern portion of the study area south of Honokawai. Most of the lower portions of the streams are perennial in nature, leaving the stream beds dry during most of the year with flow at the lower

Fig. 2. Maps showing the morphology of the study area relative to the location of known reefs and data acquisition: (a) USGS 10 m DEM showing the terrestrial morphology and the location of major drainages relative to the approximate areas of known active dense coral growth from our own observations and those by Gibbs et al. (2005); and (b) location of VM-ADCP transects along with nearshore bathymetry from SHOALS LIDAR and multibeam data. CTD/OBS profiles were taken at both the onshore and offshore ends of each VM-ADCP transect.

elevations occurring only during periods of heavy rain typically during the winter months (Soicher and Peterson, 1996).

3. Methods

The hydrographic data used in this study were collected off West Maui in the Pailolo and Auau Channels between the Hawaiian Islands of Maui, Lanai and Molokai (Figs. 1 and 2) from the R/V *Alyce C*. The data collection spanned the nearshore region from Honolua Bay south to Lahaina. Eleven shore-normal transects and one shore-parallel transect were entered into DGPS-equipped real-time positioning and mapping software before the cruise departed to make it possible to accurately re-survey the transect lines. All of the surveys were collected on the inner shelf, generally shallower than the 40 m isobath. These surveys extended inshore, usually between the 4 and 10 m isobath depending on the wave conditions. The order that the lines were surveyed (from north to south or from south to north) were alternated each day to allow us to sample each line at different times of the day and under different tide, wave and wind conditions. Three primary instruments were used to acquire data during these surveys. The first was a RD Instruments 600 kHz downward-looking, vessel-mounted acoustic Doppler current profiler (VM-ADCP), which was used to collect vertical profiles of current velocity and acoustic backscatter. A SeaBird SBE19+ conductivity/temperature/depth (CTD) profiler and a D&A Instruments OBS-3 optical backscatter sensor (OBS) were used to collect vertical profile data measuring water temperature, salinity and optical backscatter.

The VM-ADCP data were collected continuously along the transect lines while the vessel was traveling at approximately 2–3 knots (Fig. 2b). The VM-ADCP's transducer was mounted approximately 0.5 m below the sea surface and was set with a 0.5 m blanking distance; the bin size and ensemble interval were 1.0 m and 2 s, respectively. Due to the very low variability (<0.2%) in the speed of sound as determined from the CTD/OBS profiler data, a single salinity value was established and the temperature was updated from the VM-ADCP's onboard temperature sensor for sound speed calculations. The raw VM-ADCP data were archived and copies of the data were post-processed to remove all false data from below the seafloor, or data where the beam correlation dropped below 70%. The data were then averaged over 20 s windows to reduce the effects of wave-induced motions of the vessel on the data. The acoustic backscatter data were corrected for beam spreading and attenuation using the methodology proposed by Deines (1999). Principle axes of variance in the flow and the mean current direction were calculated for points spaced at 500 m intervals along each survey

Table 1
VM-ACDP survey statistics

VM-ADCP line number	Number of times lines were surveyed	Total number of samples[a]	Number of principle axis computations per line	Number of samples per principle axis computation
2	5	228	3	76
4	5	251	3	84
6	5	262	4	66
8	5	250	3	83
10	5	154	2	77
12	4	182	3	61
14	4	285	5	57
16	4	129	3	43
20	4	267	4	67
22	2	95	3	32
30	3	290	5	58
Min	2	95	2	32
Max	5	290	5	84
Mean	4	206	3	62
Standard deviation	1	67	1	16

[a]Number of 10 bin-averaged samples collected along the survey line over all the days of surveying.

line. These calculations used all of the 20 s averaged data from all of the surveys made along each specific survey line within a 500 m radius of the initial point of calculation. Because each transect was surveyed with the VM-ADCP on average four times, and current measurements (20 s averages of 2 s data) were made roughly every 15 m along each transect, the principle axes of variance in flow were computed, on average, from more than 62 averaged observations (Table 1). In trying to understand the spatial nature of the flows over the inner shelf off west Maui, previous studies (Flament and Lumpkin, 1996; Storlazzi and Jaffe, 2003) suggested that tides, wind and waves were the dominant mechanisms driving flow over and around the reefs in the study area. Consequentially, we did not employ numerical models to filter out the winds, tides or waves as one would often do when attempting to isolate specific flows (subtidal currents, etc.).

The CTD/OBS profiles were collected at the beginning and end of each VM-ADCP transect, with one cast at the inshore end of each line and one at the offshore end of each line. Other CTD/OBS profiles were collected at points along the line when interesting hydrographic features were observed. Thus a minimum of two CTD/OBS profiles were collected at each ADCP profiling line in order to relate water column structure to current velocities. The raw CTD/OBS data were archived; copies of the data were post-processed by averaging the data over 0.5 m depth windows to reduce high-frequency noise. All of the spurious data marked by a flag in the raw data were removed for visualization and analysis. The position information from the DGPS-equipped real-time positioning and mapping software was fed directly into the computers used to acquire the VM-ADCP and CTD/OBS data so that the measured quantities were georeferenced in real-time.

Meteorologic data were obtained during the study using a NovaLynx WS-16 weather station mounted approximately 40 m above sea level on top of a hotel at Honokawai. Wind speed, wind direction, relative humidity, barometric pressure and precipitation were recorded by the station every half hour. Observations of wind speed were made along each transect using a hand-held anemometer to determine the alongshore gradient in wind speed relative to the fixed measurements made by the weather station. Please see Storlazzi et al. (2003) for more details on instrumentation, data acquisition and processing methodology.

4. Results

Five days of data were acquired from 06/30/2003 to 07/04/2003 to sample currents from spring to neap tide conditions. The survey period was timed to coincide with a large-scale experiment investigating coral spawning of West Maui that included eight fixed oceanographic instrument packages, numerous drifter deployments, and biologic sampling (Storlazzi et al., 2003, 2004b). The deployment of these long-term packages allowed us to put the temporally limited but spatially extensive data presented here in the context of the long-term but spatially limited in situ instrumentation deployed between 2001 and 2003 (Storlazzi and Jaffe, 2003). For reference, the range of environmental conditions measured by the fixed stations (Storlazzi et al., 2004b) during the survey period were similar to those observed by Storlazzi and Jaffe (2003) off west Maui over the course of 15 months, allowing us to feel confident that the temporally limited spatial observations presented here have a very high probability of accurately characterizing this area's coastal system.

The location of VM-ADCP transects and CTD/OBS profiles are shown in Fig. 2b and the wind forcing and tidal stages for the study period are shown in Fig. 3. Overall, more than 99% of the data were recovered from both the VM-ADCP and CTD/OBS. Roughly 68 km of VM-ADCP data were collected from 1 m below the surface to a maximum depth of 40 m during the 5 days of surveying. The minimum, maximum and mean trackline lengths over which VM-ADCP data were collected were 253, 1897 and 997 m, respectively. Although some of the VM-ADCP data were affected by the heave, pitch and roll of the vessel when large ocean surface waves were encountered, data quality was generally high, with rare minimal losses occurring near the surface ($\leqslant 1$ bin) and near the bed (1–2 bins). The VM-ADCP data near the surface displayed slightly lower correlation due to surface wave–bubble interference with the transducers, while most of the near-bed data showed low beam correlation due to beam spreading and vessel roll. This loss of data from the bins closest to the bed is common to most mobile, downward-looking VM-ADCP surveys and was expected. The loss of acoustic data due to wave–bubble interference has also been noted by McManus et al. (2003). An example of the post-processed VM-ADCP data collected along Survey Line #14 off Mala Wharf on

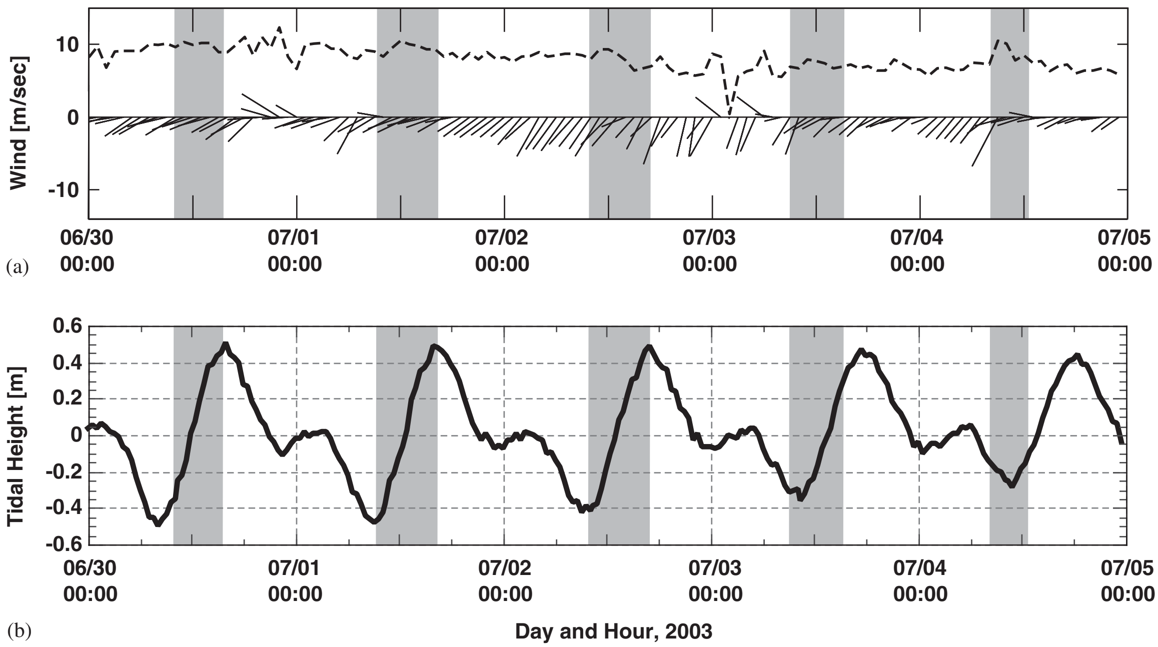

Fig. 3. Meteorologic and oceanographic forcing data during the study relative to the periods of data acquisition: (a) wind data from the USGS weather station at Honokawai, with the wind speed displayed as a dotted line and the wind velocity and direction shown as vectors; and (b) tidal data from Lahaina. The gray bands denote times of shipboard data acquisition.

07/01/2003 is shown in Fig. 4. These data show a common configuration, with northward flow over the deeper portions of fore reef and inner insular shelf and southward flow inshore over the shallower (<15 m) portions of the reef. The higher acoustic scattering at closer to shore and at depth corresponded with visually and optically (OBS data; not shown) more turbid water.

In total, 96 CTD/OBS casts were collected over the 5 days of surveying; the minimum, maximum and mean cast depths over which CTD/OBS profiler data were collected were 4, 43 and 15 m, respectively. The CTD/OBS data were high in quality, with features such as low-salinity surface plumes, multi-layered density structures and turbid layers. However, the CTD/OBS data occasionally displayed spikes in the OBS data due to interaction of the optical beam with the side of the vessel or the seafloor. These data were flagged and removed from the analyses.

Co-located laser in situ scattering and transmissometry (LISST) data acquired on 07/02/2003 showed wide spatial and temporal variability in the size of the material that was imaged by the OBS (J. Harney, personal communication). Due to this variability, we were unable to calculate a valid regression that would allow us to accurately determine suspended sediment concentrations by mass (e.g. mg/l) for the entire survey period and thus only raw OBS voltages are discussed in this paper. Examples of data from CTD/OBS profiles collected along the study area are shown in Fig. 5. These profiles show the dominant cross-shore and vertical variations in water column properties: turbid, low-salinity and low-temperature surface plumes due to stream discharge inshore and a stable, two-layer water column structure offshore.

4.1. Winds and waves

Mean wind speeds ± one standard deviation recorded by the USGS weather station at Honokawai were 6.42 ± 0.41 m/s during surveys, with the winds consistently out of the northeast. Due to orographic steering, these winds struck the west Maui shoreline from the north and northwest and decreased from the maximum velocities at the northern end of the study area to less than 1 m/s around Lahaina in the south. The northern portion of the study area off West Maui was impacted by small (H_s~0.3 m), short-period (T_d~7 s) Trade wind waves; these waves' direction was obliquely onshore to the southeast (Storlazzi et al., 2004b). The southern portion of the study area, however, was

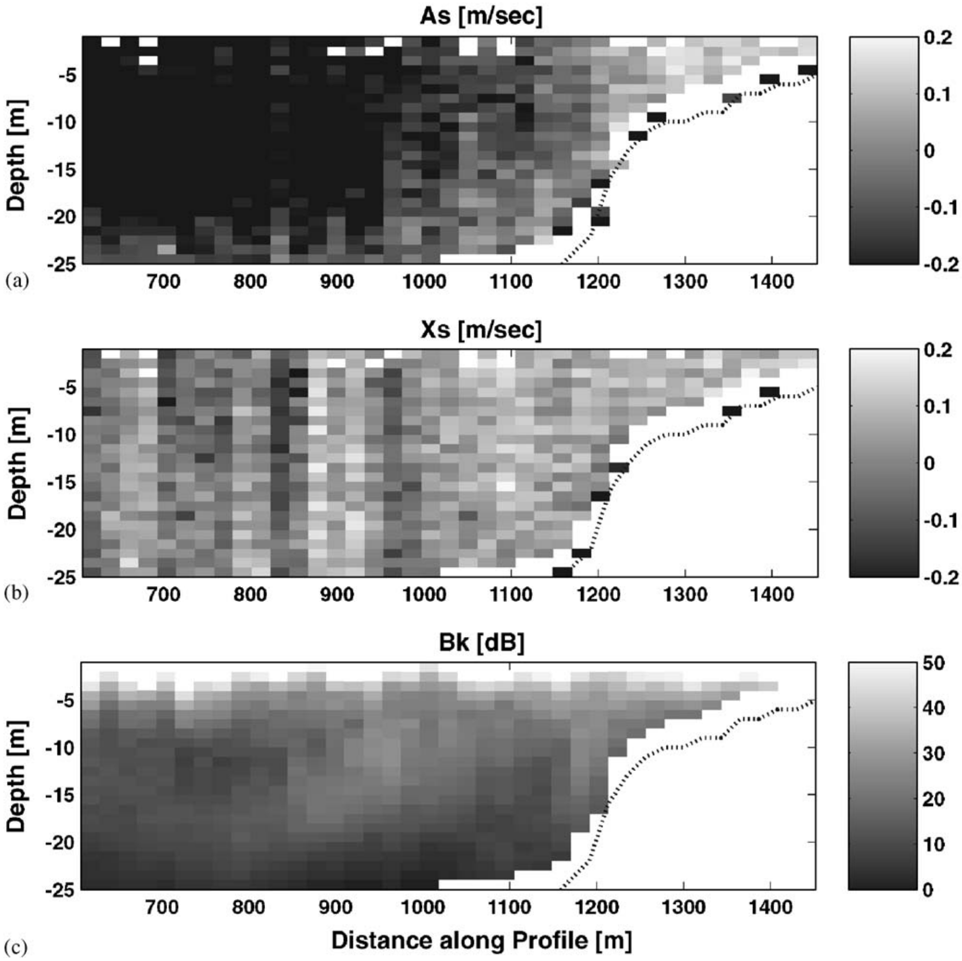

Fig. 4. Example of VM-ADCP profile data collected off Mala Wharf (Line #14) on 07/01/2003 during a falling tide: (a) alongshore to south component of current velocity; (b) onshore component of current velocity; and (c) acoustic backscatter. These data show northward flow over the deeper portions of fore reef and inner insular shelf and southward flow inshore over the shallower (<15 m) portions of the reef. The higher acoustic scattering closer to shore and at depth corresponded with visually and optically (OBS data; not shown) more turbid water.

impacted by longer-period (T_d~12 s) southern swell with similar wave heights; these waves' direction was obliquely onshore to the northeast. The wave heights off Kaanapali in the middle of the study area had extremely low wave heights (H_s~0.1 m) with short period (T_d<5 s). These wave patterns were very similar to those observed by Storlazzi and Jaffe (2003) over the previous 15 months. Also of note is that the deep-water wave heights recorded by the Waverider buoy #51202 off Mokapu Point, Oahu, HI (University of Hawaii, 2004) during the surveys varied very little, with a standard deviation in $H_s = 0.25$ m. Thus, during the study period there was an alongshore gradient in wave energy off West Maui, with the northern portion of the study area being impacted by waves out of the north and the southern portion of the study area impacted by waves out of the south; the central portion of the study area between Kaanapali and Mala Wharf received relatively little wave energy during the study.

4.2. Currents

Current speeds measured in the water column ranged from 0.01 to 1.96 m/s, with a mean ± one standard deviation of 0.24 ± 0.23 m/s (~0.9 km/h). The alongshore current speeds were typically an order of magnitude larger than the cross-shore current speeds. Assuming alongshore flow remained constant, the mean alongshore current speed of 0.25 m/s measured along the 20 m isobath would

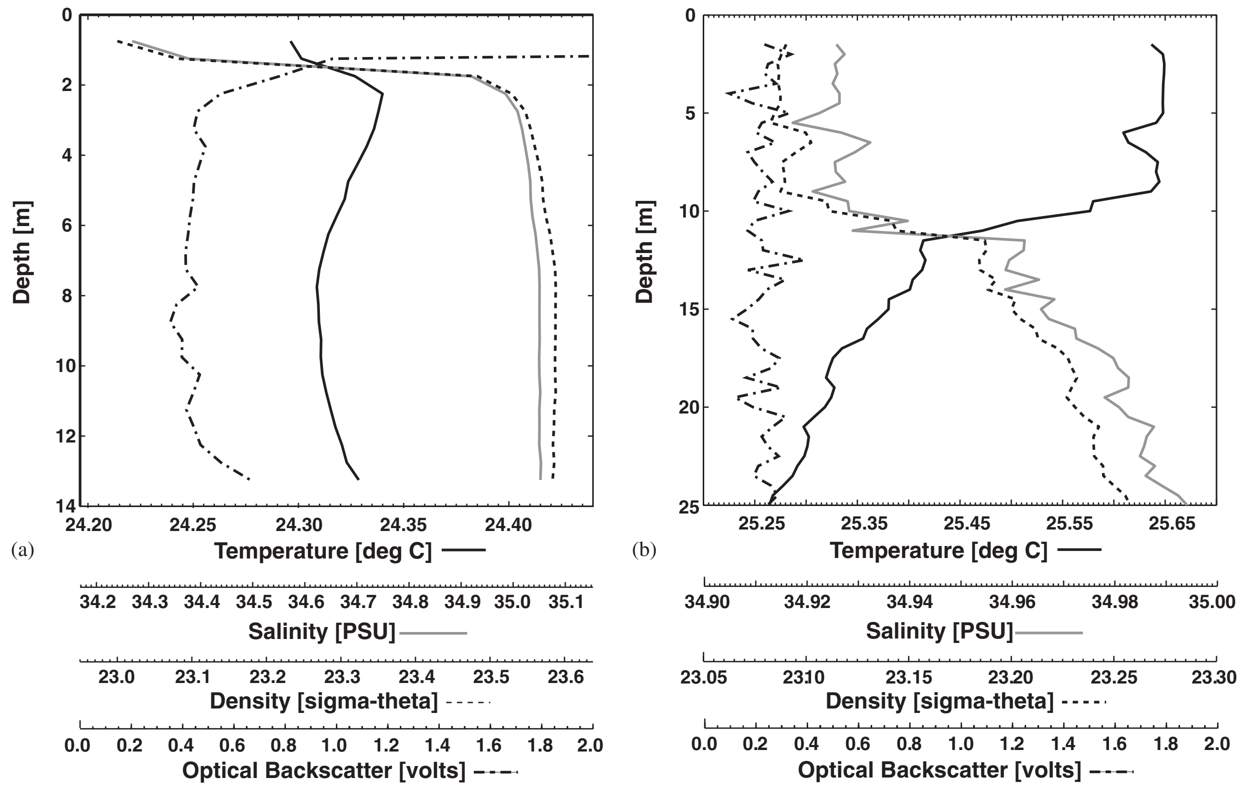

Fig. 5. Examples of data from CTD/OBS profiles collected along the study area: (a) profile collected at the inshore end of Line #20 in Honolua Bay on 07/01/2003; and (b) profile collected at the offshore end of Line #4 off Kahana on 06/30/2003. Note the different scales of the *y*-axis. The profile in Honolua Bay was taken the day after it rained; a turbid, low-salinity and temperature freshwater surface plume is evident in the data due to stream discharge. The profile taken off Kahana shows a stable, two-layer water column structure with a thermocline at a depth of approximately 10 m.

result in a total replacement of water in the 22 km long study area between Honolua Bay and southern Lahaina in just over 24 h. A mean flow of 0.10 m/s measured along the 5 m isobath would result in a total replacement of water in the study area in just over 72 h. Due to the fact that oscillatory tidal flows enhance these mean flow speeds, the actual replacement time would be shorter, as discussed by Flament and Lumpkin (1996).

Along the relatively straight sections of the coast, the flows closer to shore were typically downwind, to the south in the northern part of the study area between Kahana and Honokawai and to the north in the southern part of the study area between Mala Wharf and Lahaina. Further offshore, the currents typically flowed in the opposite direction of those inshore, to the north off the northern part of the study area between Kahana and Honokawai and to the south in the southern part of the study area between Mala Wharf and Lahaina. In Honolua Bay and in the embayment between Kaanapali and Mala Wharf, the current directions were much more irregular, generally slowly varying from one direction to another. These differences in flow direction are addressed in greater detail in the following sections.

4.2.1. Zones of cross-shore current shear

Zones of high cross-shore horizontal velocity shear, defined as (a) a change in horizontal flow direction greater than 120° in less than 50 m distance along the survey line, or (b) a change in current speed greater than 15 cm/s in less than 50 m distance along the survey line, were observed along all of the survey lines (Fig. 6). Of the 37 times that zones of high cross-shore horizontal shear were observed, 81% were due to due to flows oriented in opposite directions alongshore; the other 19% were due to strong gradients in velocity without a significant change in current direction. These zones of shear were typically observed between the 5 and 30 m isobaths along relatively straight sections of the

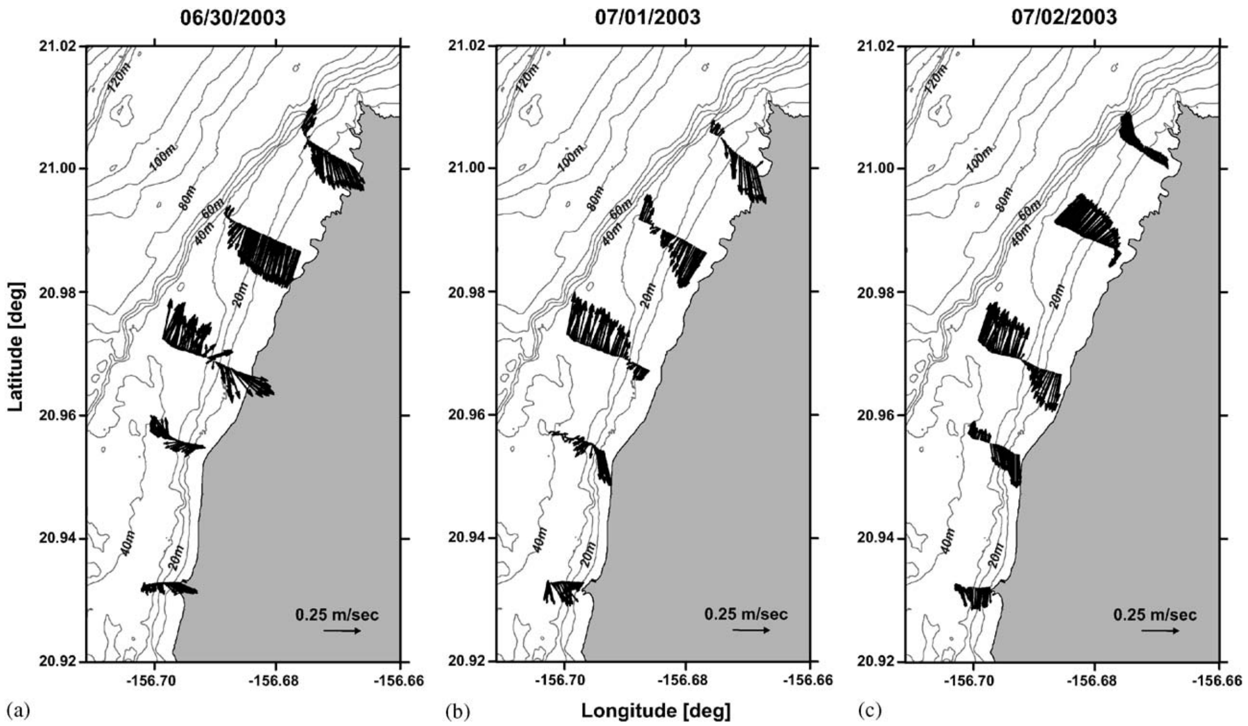

Fig. 6. Examples of zones of high cross-shore velocity shear during the study from depth-averaged VM-ADCP data collected along adjacent survey lines in less than 2 h time: (a) data collected on 06/30/2003; (b) data collected on 07/01/2003; and (c) data collected on 07/02/2004. These data show a relatively persistent zone of high cross-shore shear that parallels the reef and extends more than 2 km along the coast.

coast and corresponded to inflection points in the cross-shore bathymetry, either at the reef crest (shallower) or the base of the reef (deeper). These zones were often identifiable visually, being marked by a line of foam, debris and/or a strong change in water color, with more turbid water generally inshore of clearer offshore water. The cross-shore locations of these zones of high horizontal velocity shear were relatively stable throughout the period of study, being further offshore along Survey Lines #4 and #14 than along Lines #2, #6, #8 and #16 (Fig. 2b).

4.2.2. Eddies

Eddies, defined a change in horizontal flow direction greater than 120° in more than 100 m distance along the survey line, were often observed in the major embayments along the study area: at Honolua Bay (Fig. 7a and b) and between the headlands at Kaanapali and Mala Wharf (Fig. 7c). Flow speeds in these eddies ranged from 0.03 to 0.93 m/s and they ranged in scale from approximately 0.5 to 1.5 km across. Unlike large-scale eddies in the open ocean, these were relatively transient features that appeared to grow, decay and change their direction of rotation as the alongshore current speeds and directions changed with the tides. The eddy in the embayment between Kaanapali and Mala Wharf (Fig. 7c) was often visually identifiable, being marked by large upwelling boils, foam and debris. Overall, of the 41 total times the 11 different lines were surveyed, zones of high cross-shore horizontal shear and eddies were observed 37 times (90%). The probability of observing these features along a given survey line ranged from 100% of the time along most of the lines to 50% of the time along Line 10 off Black Rock at Kaanapali (Fig. 6d).

4.2.3. Mean flow and variability

The principle axes of variance in the flow shown in Fig. 8a are generally oriented alongshore. In a number of locations, such as the embayments between Honolua and Kapalua and between Kaanapali and Mala Wharf, the major axes are not oriented parallel to shore, but rather obliquely and the difference between the major and minor axes become less well defined close to headlands. In the

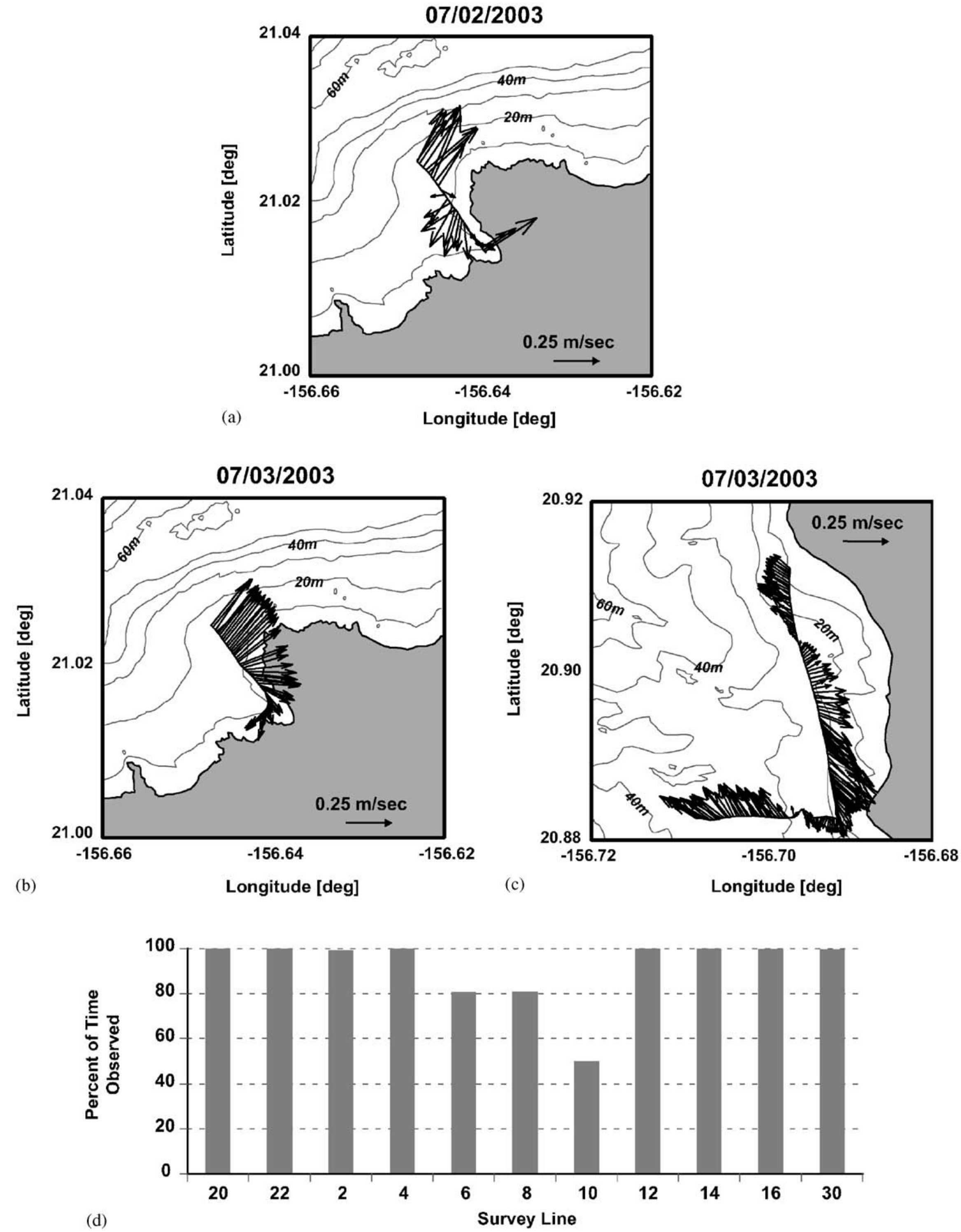

Fig. 7. Examples of eddies from depth-averaged VM-ADCP data and the distribution of eddies of zones of high cross-shore velocity shear: (a) data collected in Honolua Bay on 07/02/2003; (b) data collected in Honolua Bay on 07/03/2003; (c) data collected in the embayment between Kaanapali and Mala Wharf on 07/03/2003; and (d) plot showing the spatial distribution and frequency of observation of eddies and zones of high cross-shore shear observed during the survey period.

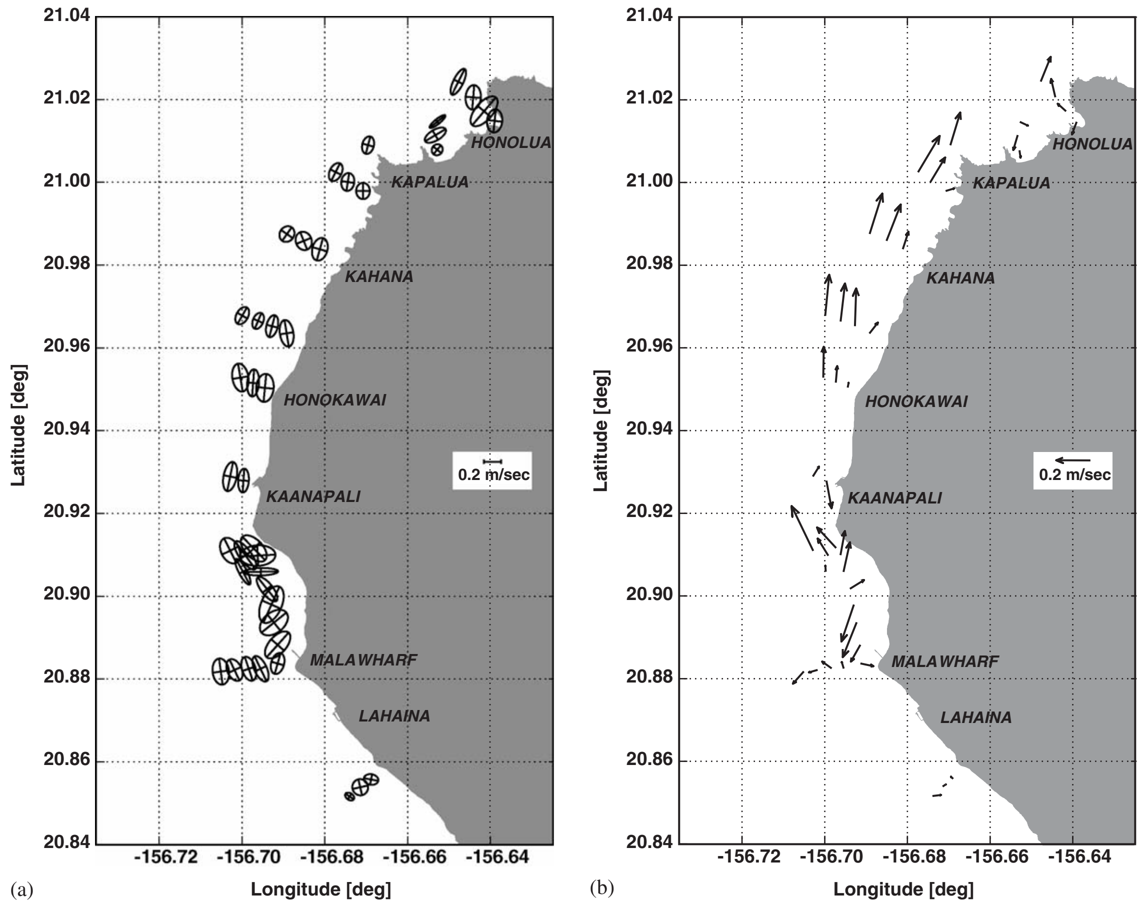

Fig. 8. Statistical analysis of currents in the study area from the 20 s averaged VM-ADCP measurements: (a) principle axes of variance in flow; and (b) the magnitude and direction of mean flow. The data display primarily alongshore flow except in the embayments between Kapalua and Honolua and between Kaanapali and Mala Wharf where the flow is more variable due to the presence of semi-permanent eddies. Mean flow is generally stronger in the northern half of the study and further offshore.

embayment between Kaanapali and Mala Wharf, flows during the individual surveys were often observed to converge or diverge, causing large eddies to form; as stated earlier, these eddies could be observed from the survey vessel. In other areas, such as off Kahana and Kapalua, the difference between the major and minor axes becomes less well defined due to strong cross-shore horizontal velocity shear. These were locations where fronts were typically observed in the individual surveys and marked by foam lines, with the flow observed to change approximately 180° in orientation (generally from northeast to southwest, or vice versa) during the period of data acquisition along the survey line.

The mean currents observed in the study area during the surveys (Fig. 8b) varied in the both the cross-shore and alongshore directions. Since the data from the different surveys were averaged over a 500 m radius to compute the mean flow vectors, much of the flow closes to shore over the shallower portions of the reefs, which was often heading in the opposite direction of the flow further offshore, was averaged with the offshore flow. This spatial and temporal averaging across these zones of high cross-shore horizontal shear resulted in small net mean current vectors being calculated close to shore and a loss of our ability to image the narrow inshore jets over the shallower portions of the reefs heading in the opposite direction of the offshore flow. This averaging does, however, increase the statistical weighting of the data to help us better understand the nature of the larger scale flow patterns in the study area. Overall, mean current speeds were typically greater further offshore (~0.25 m/s) except off the headland at Kaanapali and in the embayment between Kaanapali and Mala Wharf; the lowest mean current speeds (~0.05 m/s) were observed off southern Lahaina. Net flow along the offshore ends of the survey lines in the northern part of the study area between Honokawai and Honolua Bay was uniformly to the northeast, while the flow closer to shore was significantly reduced in intensity due to the spatial averaging discussed above. Conversely, at the offshore ends of the survey lines off Mala Wharf and southern Lahaina the mean currents were to the south, while closer to shore they were reduced in intensity, also due to the spatial averaging discussed above. Similar to the principle axes of variance in flow, the mean current vectors in the embayments between Honolua and Kapalua and between Kaanapali and Mala Wharf were not oriented shore-parallel. The mean current vectors in the bays between Kapalua and Honolua suggest the presence of two, semi-permanent eddies, with one along Survey Line #22 off DT Fleming State Beach in Kapalua and one along Survey Line #20 in Honolua Bay (Fig. 2b). In the embayment between Kaanapali and Mala Wharf, a number of large cyclonic and anti-cyclonic eddies were observed. The spatial and temporal averaging of these features resulted in net mean flows suggesting divergence in the middle of the embayment and flow convergence at the headlands at Kaanapali and Mala Wharf. We are not sure, however, how accurately these computed vectors represent the true nature of mean flows in this region due to the high temporal variability in the flow directions at these locations.

4.3. Water column properties

The water column properties that were collected included temperature (°C), salinity (PSU) and raw optical backscatter (V) with depth; from the temperature and salinity data we were able to compute density (σ_t) and the speed of sound in the water column (υ). The mean, minimum, maximum and standard deviation in temperature, salinity, optical backscatter and density at both the inshore, shallow end and deep, offshore end of each survey line are listed in Table 2. The temperature, salinity and raw optical backscatter measurements are discussed in the following sections.

4.3.1. Temperature

Temperature stratification (not shown) was generally relatively low (typically < 0.5 °C) and was greater further offshore, with the observed depth of the thermocline typically between 10 and 25 m. The absence of a thermocline further inshore was likely due to two factors: shallow depth (less than 20 m) leading to increased tidal mixing and mixing by surface waves. Often, the water column close to shore was comprised of cool surface water overlying warm near-bed water. This thermal inversion was probably related to freshwater discharge from the adjacent stream mouths.

Table 2
Statistics of water column properties from the CTD/OBS profiles

Parameter		Deep[a]	Shallow[b]	All
Temperature (°C)	Mean	25.566	25.635	24.984
	Minimum	24.702	24.993	22.918
	Maximum	26.513	27.557	27.557
	Standard deviation	0.263	0.360	0.266
Salinity (PSU)	Mean	34.934	34.870	34.957
	Minimum	34.727	33.572	33.572
	Maximum	35.078	35.012	36.296
	Standard deviation	0.048	0.111	0.081
Density (σ_t)	Mean	23.119	23.049	23.313
	Minimum	22.737	22.258	22.258
	Maximum	23.490	23.312	24.475
	Standard deviation	0.115	0.135	0.109
OBS (V)	Mean	0.234	0.646	0.444
	Minimum	0.000	0.111	0.000
	Maximum	3.349	4.705	4.705
	Standard deviation	0.108	0.580	0.294

[a]Data from casts taken at the offshore ends of the survey lines (water depth > 15 m).
[b]Data from casts taken at the inshore ends of the survey lines (water depth < 10 m).

The map of depth-averaged mean temperature for each profile in the study area displays a general 0.5–1.5 °C increase in temperature from north to south (Fig. 9a). In the northern half of the study area, warmer water was typically observed further from shore; the near-shore low temperatures are likely related to cool, fresh groundwater flowing out of streams or submarine groundwater discharge percolating out of the reef, which was often observed in the field during snorkeling and scuba dives as "shimmering water" caused by the different indices of refraction related to the separate water mass's densities. As previously mentioned, the uplands along the northwestern section of Maui above Honolua south to Kahana typically receive higher precipitation than the uplands further to the south due to orographic effects associated with the West Maui shield volcano. Thus, infiltration and groundwater effluence on the reef are more likely to

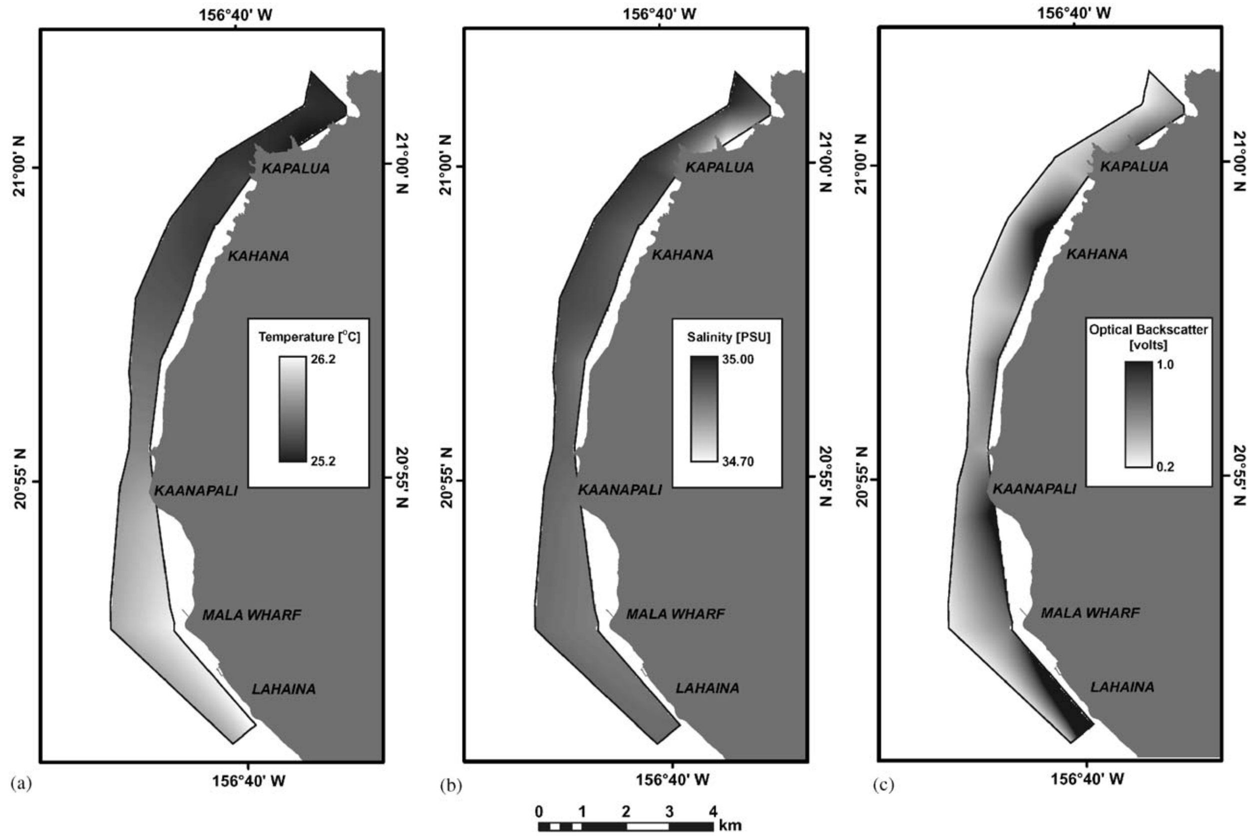

Fig. 9. Maps of depth-averaged water column properties in the study area: (a) mean temperature; (b) mean salinity; and (c) mean turbidity. The temperature data show an alongshore temperature gradient on the order 1 °C, likely caused by solar insolation and less Trade wind wave-induced mixing in the south. Salinity is typically lower closer to shore due to freshwater runoff from streams and groundwater effluence through the reef. Optical backscatter is typically quite low except in areas affected by turbid stream discharge or wave-induced resuspension of seafloor sediment. Most of the regions where lower salinities and higher turbidities are typically observed are correlated with significant terrestrial drainages and either the absence or poor health of coral reefs.

occur along the northern section of the study area. In the southern half of the study area, however, the warmest water temperatures were typically observed closer to shore, which would be consistent with increased warming of the shallower water column onshore due to solar insolation during the daytime and its mixing with cooler water further offshore out in the Auau Channel.

4.3.2. Salinity

Profiles of salinity were typically stable, with lower salinity surface waters overlying higher salinity near-bed waters. In a number of the profiles close to shore, however, the near-bed salinity was lower than the near-surface salinity. These inverted profiles are likely due to the effluence of freshwater from the shoreline via subsurface seeps. The calculated densities in these profiles reveal near-bed density instabilities as a result of this low salinity water. Thus, extensive mixing was occurring in the bottom few meters of these profiles.

The maps of mean, depth-averaged salinity for each cast in the study area are shown in Fig. 9b. In general, the salinity along West Maui varies less than 0.25 except locally at the mouths of streams. The lower salinity water observed close to shore was generally lower in temperature (Fig. 9a). Low temperature, low salinity water was most likely related to greater freshwater discharge out of the well-developed drainages directly onshore or from submarine groundwater discharge from the upper shoreface. Specifically, the low nearshore salinities observed off Kapalua and Honolua are likely due to the frequent summertime Trade wind-induced orographic showers on the northern portion of the West Maui volcanic cone.

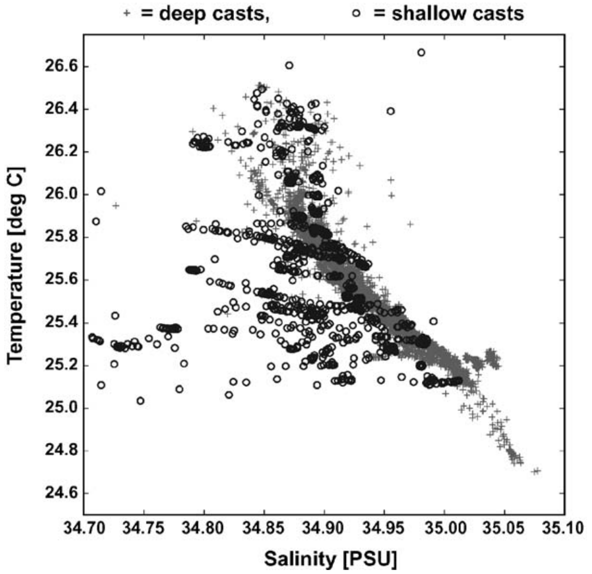

Fig. 10. Relationships between temperature and salinity. The data from the deeper, offshore casts show a more common inverse temperature–salinity relationship. The shallower data, however, show greater scatter due to the greater influence from terrestrial freshwater input, solar insolation and wave-induced mixing.

A temperature–salinity (T–S) plot for the cruises is shown in Fig. 10. The data from the deeper profiles display the typical decrease in temperature with increasing salinity. This trend is indicative of less mixing and a stable water column: warm, low salinity water overlying cooler, more saline water. The cooler, more saline values are likely due to either weak wind-driven upwelling or tidal pumping as observed by Storlazzi and Jaffe (2003). The lower temperature and salinity values in the shallower profiles result from freshwater effluence through the reef or direct runoff from streams while the uniform temperatures in the shallower profiles most likely result from wave and tidal mixing and high temperature diffusivity.

4.3.3. Optical backscatter

The maps showing the distribution of optical backscatter in the study area display high spatial heterogeneity (Fig. 9c). The high optical backscatter features in the northern part of the study area were caused by higher-than normal suspended sediment loads related to freshwater plumes discharged from streams as shown in the salinity data (Figs. 9b and 10) and kept in suspension by Trade-wind waves. The long-period waves out of the south resuspended fine-grained bed sediment off the south-facing

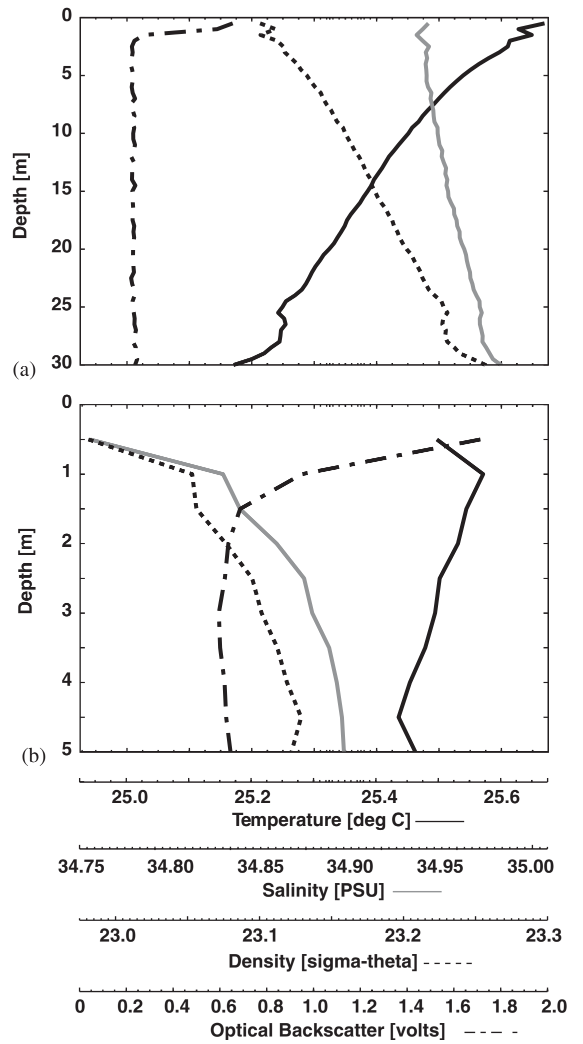

Fig. 11. Plots of mean vertical variation in water column properties in the study area: (a) profiles taken at the offshore ends of the survey lines; and (b) profiles taken at the inshore ends of the survey lines. Note the different scales of the y-axis. Turbidity is typically higher and salinity and temperature are lower right at the surface due to freshwater runoff close to shore. Turbidity and temperature then decrease with depth as salinity increases closer to the bed. As discussed in Fig. 10, salinity is lower and turbidity is higher closer to shore.

sections of the coast at Lahaina and Kaanapali, likely deposited during the previous winter's storms, causing high optical backscatter.

4.3.4. Variability in water column properties with depth

The overall trend for the variation in water column properties with depth indicated turbid buoyant freshwater plumes inshore and a stable water column with vertical structure offshore (Fig. 11).

Overall, temperature and optical backscatter decreased with depth while salinity and density increased with depth. At the very surface of the inshore ends of the survey lines, higher backscatter but lower temperature, salinity and density are indicative of the influence of turbid buoyant freshwater plumes from stream discharge. The temperature typically quickly rose to its maximum within a meter of the surface, and then decreased slowly towards the bed. Optical backscatter generally decreased logarithmically towards the bed, reaching base levels approximately 2 m below the water's surface; this suggests the slow settling of scattering material from the surface plume. The low salinity and density near the surface also support the presence of a buoyant freshwater surface plume, similar to that observed in individual casts (Fig. 5b).

Further offshore, the effects of the turbid buoyant freshwater surface plumes can still be identified by their lower salinity and density along with the higher optical backscatter. More important, however, were the presence of vertical (layered) structures in the water column that were clearly identified in the individual profiles (Fig. 5a) but are manifested in the mean profiles (Fig. 11) as a general decrease in temperature and increase in salinity and density with depth due to the spatial variability in the depth of the thermocline. The temperature and salinity differences between the overlying warmer, less saline water mass and the cooler, more saline water mass were often on the order of 0.25 °C and 0.15, respectively. Numerous times during the surveys large, rapid displacements in the temperature, salinity and density profiles were observed at depths between 10 and 25 m, suggesting the presence of internal waves or non-linear internal tidal bores, similar to those observed in the long-term instrument deployment off Kahana, Maui from the fall of 2001 through the spring of 2003 (Storlazzi and Jaffe, 2003).

5. Discussion

These analyses, in conjunction with field observations and long-term, fixed instrument deployments (Storlazzi and Jaffe, 2003; Storlazzi et al., 2004a, b) evoke the following conceptual model of meteorologic and oceanographic processes over the inner shelf off West Maui. The Northeast Trade winds striking the West Maui volcanic cone cause a strong north–south gradient in precipitation along West Maui throughout the year. This precipitation gradient, along with the large area of plowed agricultural lands on the uplands in this area causes, on average, more freshwater and sediment to be discharged from streams in the northern part of the study area between Honolua Bay and Kahana than further south. This stream discharge, along with submarine groundwater discharge, causes lower salinities and higher fine-grained suspended sediment concentrations close to shore. The frequent lower nearshore salinities caused by this freshwater discharge might stress corals in this area, similar to the findings of Jokiel et al. (1993). As discussed by the West Maui Watershed Management Project (1996) and Dollar and Andrews (1997), the terrestrial groundwater being discharged into the nearshore typically has elevated nutrient loads. Most of this sediment-rich, lower salinity water is driven south alongshore over the shallower portions of the reefs due to Trade winds, wave-induced breaking and the resulting wave-driven currents. These flows appear to keep the plumes coherent alongshore, reducing dissipation by forcing the plumes against the shoreline while the wave-generated turbulence tends to keep the fine-grained sediment in suspension, offsetting the plume's settling due to gravity. Together, these two factors persistently create relatively high turbidities close to shore in the Kahana region.

The turbid, lower-salinity, southward-flowing inshore jet over the shallower portions of the reefs in the northern part of the study area appears to veer offshore between Honokawai and Kaanapali, although it is not clear exactly where this occurs due to the highly variable currents measured in this area. Observations by our group and others (E. Brown, personal communication; West Maui Watershed Management Project, 1996; Dollar and Andrews, 1997) have shown that coral health is quite poor along this section of coast, with low coral coverage and high macroalgal growth that is indicative of high nutrient loading. It has not, however, been assessed whether the poor coral health in this area is due to: (1) lower than normal salinity, or (2) nutrients from either stream discharge or submarine groundwater discharge through the shoreface.

The flow close to shore offshore of Lahaina heads north past Mala Wharf; it is not clear what happens to this inshore flow north of Mala Wharf and south of Kaanapali. The region between Mala Wharf and Kaanapali appears to be a zone of eddy formation. These eddies and the lack of large ocean surface waves due to shadowing by the surrounding islands

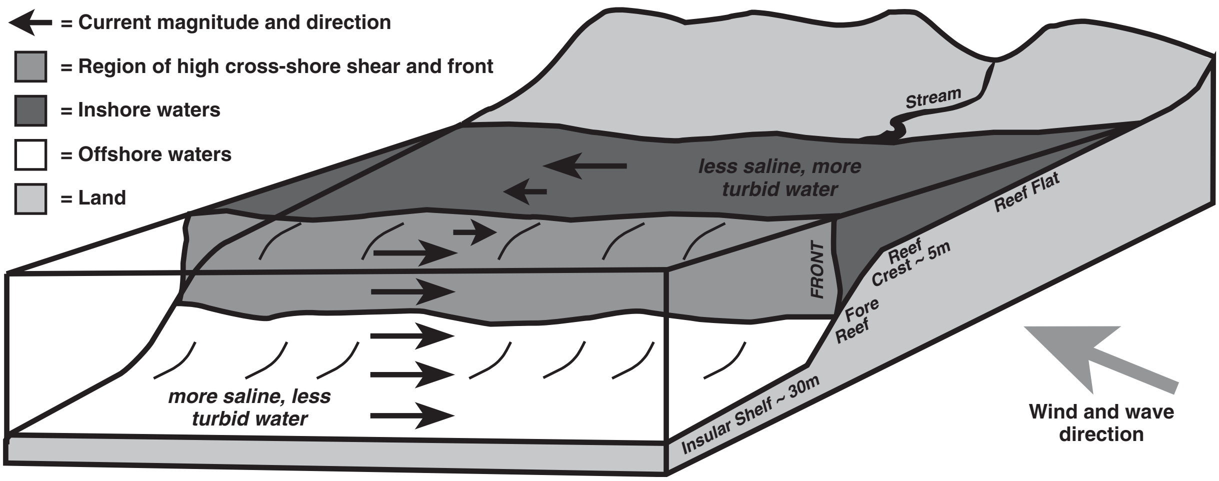

Fig. 12. Schematic of the dynamics of flow and water column properties along reefs in the study area. Higher turbidity and submarine groundwater discharge or freshwater runoff is typically found close to shore. Along the relatively straight sections of coast, net wave- and wind-driven flow close to shore is downwind. Flow further offshore is upwind, causing zones of high cross-shore horizontal velocity shear and often fronts.

help to retain fine-grained sediment in this area, causing persistent high turbidity in the absence of high fluvial discharge. Similar retention of turbid freshwater water likely does not occur in Honolua Bay during the winter when stream discharge is the greatest due to the rapid flushing and mixing of the bay as it is impacted by large North Pacific storm waves.

Our observations suggest the reefs off West Maui can be broken down into two sections based on the dominant mechanisms driving flow (Fig. 12). Over the shallower portions of the reef like the reef crest and reef flat, asymmetrical surface wave orbital motions due to shoaling and wave breaking-induced currents dominate, as discussed by Storlazzi and Jaffe (2003); these appear to be the primary control on flow when the water depth is small relative to the size of the wave-orbital motions and the wind-driven surface layer. Further offshore where the water depth is much greater than the size of the wave motions and the wind-drive surface layer, longer period tidal and subtidal current appear to dominate the flow. Both Ogston et al. (2004) and Storlazzi et al. (2004a) observed similar phenomena of the extensive fringing reef off south-central Molokai. When the tidal and/or subtidal flow opposes the wave- and wind-driven surface flow, a zone of high cross-shore horizontal shear and thus vorticity is formed, similar to that observed in Figs. 4a and 6. As shown in Figs. 9 and 10, inshore of these zones of high cross-shore shear, the waters were typically less saline and more turbid, while offshore of these shear zones the waters were more saline and less turbid. These cross-shore variations in flow and water properties, along with the often visible accumulation of foam or debris in a shore-parallel line at the location of the change in sign of alongshore flow, suggest that these regions were often the position of a front. Due to the lack of CTD/OBS profiler data just to either side of these regions, we are unable to quantitatively document the magnitude of the horizontal gradients of the hydrographic properties to determine the nature of the fronts.

The regions with high cross-shore horizontal shear and eddies were typically observed between the 5 and 30 m isobaths along the study area, which is intriguing. The relatively persistent location of these features along the survey lines correlate with the reef crest (minimum depth) and base of the reef (maximum depth), respectively, in the study area. It is impossible for us to determine whether the presence of the reef topographically steers the flow and forces the location of this front or if the presence of this front defines where these inflection points in the reef are located. In either case, however, it has been shown in numerous other locations that such zones of velocity shear or fronts often help to retain particulate matter, phytoplankton and many larval species (e.g. Alldredge and Hamner, 1980; Mann, 1988; Franks, 1997; Pineda, 1999; Flament and Armi, 2000; Dekshenieks et al., 2001). In the case of Honolua Bay, we conclude that the persistent eddy feature may help to retain coral larvae during the summer spawning season when North Pacific winter storm waves and wave-induced mixing is relatively minor. Furthermore, the cross-shore horizontal velocity shear likely reduces the advection of material across these regions and causes material to be retained within the different water bodies on either side of these regions of high cross-shore shear.

While healthy reefs bound the shallow regions (depths <15 m) on northern and southern sides of the embayment between Kaanapali and Mala Wharf, the persistent eddy features in the embayment likely helps to retain fine-grained sediment transported southward along the coast or discharged from ephemeral streams in the area during the infrequent Kona storms. The resulting turbid waters may hamper substantial coral reef development due to low light availability for photosynthesis (e.g. Marszalek, 1981) or relatively high sediment accumulation rates in the absence of substantial wave energy (e.g. Dodge et al., 1974; Rogers, 1990). These persistent shear zones, and likely fronts, between the 5 and 30 m isobaths off Lahaina and the Kahana-Honokawai region may help to retain larvae in this region, promoting reef development. Conversely, these zones of high cross-shore horizontal shear might cause the nutrients and/or fine-grained sediment loads discharged from the land, which have increased in recent times due to poor land use practices, to accumulate, potentially harming the reefs by reducing light available for photosynthesis or promoting nutrient-rich algal growth (e.g. Szmant, 2002). It therefore appears that while these mesoscale oceanographic processes (zones of cross-shore horizontal hear, fronts and eddies) may not be the primary control on the location of coral reefs along West Maui, that they can concentrate or disperse dissolved and particulate matter, which can affect the health and sustainability of coral reefs. The high spatially and temporally variable currents and water column properties observed along West Maui also suggest that numerical modeling of water column properties and transport in the vicinity of reefs must take into account the nature of the fluctuations to accurately model dissolved or particulate matter flux in these types of environments.

6. Conclusions

More than 68 km of high-resolution VM-ADCP data and 96 CTD/OBS profiles were collected off northwestern Maui, Hawaii, USA during surveys conducted in the summer of 2003. Results from the study highlight the high temporal and spatial heterogeneity in flow and water column properties over a section of coast with patch and fringing reefs. We have several critical findings from both past studies and these measurements and analyses presented here.

First, wave- and wind-driven surface flows appear to be the primary control on flow over shallower (<10 m) portions of the reef while tidal and subtidal currents dominate flow over the outer portions of the reef and insular shelf. When the direction of the flows are counter to one another, which is quite common in many coastal areas, they cause a zone of high cross-shore horizontal shear and often form a front that may accumulate particulate and dissolved material in this zone and may hamper advection across the region of high shear, trapping material (water, particulate matter, etc.), to one side or the other of these regions. It is not clear whether these zones of high cross-shore horizontal shear and fronts are the cause or the result of the location of the reef, but they appear to be correlated alongshore over relatively large horizontal (orders of kilometer) distances.

Second, we find that when two flows converge or when a single flow is steered by bathymetry around headlands or in embayments, semi-permanent eddies are generated that, in the absence of large ocean surface waves, have the potential to accumulate material.

Third, we have also determined that high turbidity along the study area was generally correlated with one of two processes: large wave events that resuspend fine-grained bed sediment and cause elevated turbidity levels over long stretches of coastline, and turbid freshwater runoff that has a tendency to be more isolated along the coast in the area of stream mouths. We also find that the waters off West Maui are generally more saline and less turbid further offshore and with increasing depth. These overall trends, however, are greatly influenced by the presence of freshwater either from stream discharge or groundwater effluence through the shoreface. Finally, results from this study indicate that areas of higher turbidity and lower salinity tend to correlate with regions of poor coral health or the absence of well-developed reefs, suggesting that the oceanographic processes (e.g. mesoscale fronts and eddies) that concentrate and/or transport nutrients, contaminants, low-salinity water or suspended sediment might strongly influence reef health and sustainability.

Overall, these data demonstrate that nature of flow and particulate flux along an irregular volcanic island's shoreline can be quite complex, with flows heading in different directions along different isobaths on a given reef and the resulting biological and chemical processes that take place are likely dominated by different physical processes. Furthermore, these data provide us with a clear picture of the nature of and controls on water column properties such as temperature, salinity and turbidity whose spatial distribution and transport are often governed by flow and which play a vital role in determining coral reef development and health in the study area.

Acknowledgments

This work was carried out as part of the USGS's Coral Reef Project as part of an effort in the US and its trust territories to better understand the effect of geologic processes on coral reef systems. Project Chief Michael Field deserves thanks for providing us with the patience, opportunity and support to carry out these cruises. We would like to thank Joe Reich, the captain of the R/V *Alyce C.*, for his superb work during the long days while we surveyed at speeds too slow to fish. We would also like to thank Amy Draut (USGS) and Patrick Barnard (USGS), who contributed numerous excellent suggestions and a timely review of our work. Use of trademark names does not imply USGS endorsement of products.

References

Acevedo, R.J., Morelock, J., Olivieri, R.A., 1989. Modification of coral reef zonation by terrigenous sediment stress. Palios 4, 92–100.

Alldredge, A.L., Hamner, W.M., 1980. Recurring aggregation of zooplankton by a tidal current. Estuarine and Coastal Marine Science 10, 31–37.

Bastidas, C., Bone, D., Garcia, E.M., 1999. Sedimentation rates and metal content of sediments in a Venezuelan coral reef. Marine Pollution Bulletin 38 (1), 16–24.

Buddemeir, R.W., Hopley, D., 1988. Turn-ons and turn-offs: causes and mechanisms of the initiation and termination of coral reef growth. In: Proceedings of the Sixth International Coral Reef Congress, pp. 253–261.

Clague, D.A., Dalrymple, G.B., 1989. Tectonics, geochronology, and origin of the Hawaiian Emperor Volcanic chain. In: Winterer, E.L., Hussong, D.M., Decker, R.W. (Eds.), The Eastern Pacific Ocean and Hawai'i. The Geological Society of America, Boulder, CO, pp. 188–217.

Coles, S.L., Ruddy, L., 1995. Comparison of water quality and reef coral mortality and growth in Southeastern Kaneohe Bay, Oahu, Hawaii, 1990–1992, with conditions before sewage diversion. Pacific Science 49 (3), 247–265.

Deines, K.L., 1999. Backscatter estimation using broadband acoustic Doppler current profilers. RD Instruments Application Note FSA-008, 5pp.

Dekshenieks, M.M., Donaghay, P.L., Sullivan, D.M., Rines, J.E.B., Osborne, T.R., Twardowski, M.S., 2001. Temporal and spatial occurrence of thin phytoplankton layers in relation to physical processes. Marine Ecology Progress Series 223, 61–71.

Dickson, K.L., Maki, A.W., Brungs, W.A., 1987. Fate and Effects of Sediment-bound Chemicals in Aquatic Systems. Pergamon Press, New York.

Dodge, R.E., Aller, R.C., Thompson, J., 1974. Coral growth related to suspension of bottom sediments. Nature 247, 574–577.

Dollar, S., Andrews, C., 1997. Algal blooms off West Maui: Assessing Casual Linkages Between Land and the Coastal Ocean, Final Report. University of Hawaii, Honolulu, Hawaii 40pp.

Flament, P., Armi, L., 2000. The shear, convergence and thermohaline structure of a front. Journal of Physical Oceanography 30, 51–66.

Flament, P., Lumpkin, C., 1996. Observations of currents through the Pailolo Channel: implications for nutrient transport. In: Wiltse, W. (Ed.), Algal Blooms: Progress Report on Scientific Research, West Maui Watershed Management Project, pp. 57–64.

Fletcher, C.H., Richmond, B.M., Grossman, E.E., Gibbs, A.E., 2002. Atlas of natural hazards in the Hawaiian Coastal Zone, USGS Geologic Investigations Series I-2716.

Fortes, M., 2000. The effects of siltation on tropical coastal ecosystems. In: Wolanski, E. (Ed.), Oceanographic Processes of Coral Reefs. CRC Press, Boca Raton, FL, pp. 93–112.

Franks, P.J.S., 1997. Spatial patterns in dense algal blooms. Limnology and Oceanography 45 (5/2), 1297–1305.

Garrison, G.H., Glenn, C.R., McMurtry, G.M., 2003. Measurement of submarine groundwater discharge in Kahana Bay, Oahu, Hawaii. Limnology and Oceanography 48 (2), 920–928.

Gee, A., Bruland, K., 2002. Tracing Ni, Cu, and Zn kinetics and equilibrium partitioning between dissolved and particulate phases in South San Francisco Bay, California, using stable isotopes and high-resolution inductively coupled plasma mass spectrometry. Geochimica et Cosmochimica Acta 66 (17), 3063–3083.

Gibbs, A.E., Grossman, E.E., Richmond, B.M., 2005. Summary and preliminary interpretations of USGS cruise A202HW: underwater video surveys collected off Oahu, Molokai and Maui, Hawaii, June–July, 2002. US Geological Survey Open-File Report 2005–1244, 57pp. http://pubs.usgs.gov/of/2005/1244/

Guzman, H.M., Tudhope, A.W., 1998. Seasonal variation in skeletal extension rate and stable isotopic (C-13/C-12 and O-18/O-16) composition in response to several environmental variables in the Caribbean reef coral Siderastrea sidereal. Marine Ecology Progress Series 166, 109–118.

Harrison, P.L., Ward, S., 2001. Elevated levels of nitrogen and phosphorus reduce fertilization success of gametes from scleractinian reef corals. Marine Biology 139, 1057–1068.

Heikoop, J.M., Risk, M.J., Lazier, A.V., Edinger, E.N., Jompa, J., Limmon, G.V., Dunn, J.J., Browne, D.R., Schwarcz, H.P., 2000. Nitrogen-15 signals of anthropogenic nutrient loading in coral reefs. Marine Pollution Bulletin 21 (7), 628–636.

Jokiel, P.L., Hunter, C.L., Taguchi, S., Watarai, L., 1993. Ecological impact of a fresh-water reef kill in Kaneohe Bay, Oahu, Hawaii. Coral Reefs 12 (3–4), 177–184.

Jokiel, P.L., Brown, E.K., Friedlander, A., Rodgers, S.K., Smith, W.R., 2001. Hawaii Coral Reef Initiative Coral Reef Assessment and Monitoring Program (CRAMP) Final Report 1999–2000. University of Hawaii, Hawaii 66pp.

Kraines, S.B., Yanagi, T., Isobe, M., Komiyama, H., 1998. Wind-wave driven circulation on the coral reef at Bora Bay, Miyako Island. Coral Reefs 17, 133–143.

Lugo-Fernandez, A., Roberts, H.H., Wiseman, W.J., Carter, B.L., 1998. Water level and currents of tidal and infragravity periods at Tague Reef, St. Croix (USVI). Coral Reefs 17, 343–349.

Mann, R., 1988. Distribution of bivalve larvae at a frontal system in the James River, Virginia. Marine Ecology Progress Series 50, 29–44.

Marszalek, D.S., 1981. Impact of dredging on a subtropical reef community: southeastern Florida, USA. In: Proceedings of the Fourth International Coral Reef Congress, pp. 147–153.

M&E Pacific, 1991. Water Use and Development Plan for the Island of Maui, 1992. Draft report prepared for the Department of Water Supply, County of Maui, Hawaii.

McKenna, S.E., Richmond, R.H., Roos, G., 2001. Assessing the effects of sewage on coral reefs: developing the techniques to detect stress before coral mortality. Bulletin of Marine Science 69 (2), 517–523.

McManus, M.A., Alldredge, A.L., Barnard, A., Boss, E., Case, J., Cowles, T.J., Donaghay, P.L., Eisner, L., Gifford, D.J., Greenlaw, C.F., Herren, C., Holliday, D.V., Johnson, D., MacIntyre, S., McGehee, D., Osborn, T.R., Perry, M.J., Pieper, R., Rines, J.E.B., Smith, D.C., Sullivan, J.M., Talbot, M.K., Twardowski, M.S., Weidemann, A., Zaneveld, J.R.V., 2003. Changes in characteristics, distribution and persistence of thin layers over a 48-h period. Marine Ecology Progress Series 261, 1–19.

Merrifield, M.A., Yang, L., Luther, D.S., 2002. Numerical simulations of a storm generated island-trapped wave event at the Hawaiian Islands. Journal of Geophysical Research 107 (C10), 3169.

Moberly, R.M., Chaimberlin, T., 1964. Hawaiian Beach Systems. University of Hawaii, Hawaii.

Ogston, A.S., Storlazzi, C.D., Field, M.E., Presto, M.K., 2004. Currents and suspended sediment transport on a shallow reef flat: South-central Molokai, Hawaii. Coral Reefs 23, 559–569.

Pineda, J., 1999. Circulation and larval distribution in internal tidal bore warm fronts. Limnology and Oceanography 44 (6), 1400–1414.

Roberts, H.H., Murray, S.P., Suhayda, J.N., 1977, Physical processes in a fore-reef shelf environment. In: Proceedings of the Third International Coral Reef Symposium, vol. 2, pp. 507–515.

Roberts, H.H., Murray, S.P., Suhayda, J.N., 1980. Physical processes in a fringing reef system. Journal of Marine Research 33, 233–260.

Rogers, C.S., 1990. Responses of coral reefs and reef organisms to sedimentation. Marine Ecology Progress Series 62, 185–202.

Saouter, E., Campbell, P.G., Ribeyre, F., Boudou, A., 1993. Use of partial extractions to study mercury partitioning on natural sediment particles—a coutionary note. International Journal of Environmental Analytical Chemistry 54, 57–68.

Soicher, A.J., Peterson, F.L., 1996. Assessing Terrestrial Nutrient and Sediment Discharge to the Coastal Waters of West Maui, Hawaii. University of Hawaii, Honolulu, Hawaii 98pp.

Storlazzi, C.D., Jaffe, B.E., 2003. Coastal circulation and sediment dynamics along west Maui, Hawaii, Part I: long-term measurements of currents, temperature, salinity and turbidity off Kahana, West Maui: 2001–2003. US Geological Survey Open-File Report 03-482, 28pp. http://pubs.usgs.gov/of/2003/of03-482/

Storlazzi, C.D., Logan, J.B., McManus, M.A., McLaughlin, B.E., 2003. Coastal circulation and sediment dynamics along west Maui, Hawaii, Part II: hydrographic survey cruises A-3-03-HW and A-4-03-HW. Report on the spatial structure of currents, temperature, salinity and turbidity along Western Maui. US Geological Survey Open-File Report 03-430, 50pp. http://pubs.usgs.gov/of/2003/of03-430/

Storlazzi, C.D., Ogston, A.S., Bothner, M.H., Field, M.E., Presto, M.K., 2004a. Wave- and tidally driven flow and sediment flux across a fringing coral reef: south-central Molokai, Hawaii. Continental Shelf Research 24 (12), 1397–1419.

Storlazzi, C.D., Field, M.E., Ogston, A.S., Logan, J.B., Presto, M.K., Gonzales, D.G., 2004b. Coastal circulation and sediment dynamics along west Maui, Hawaii, Part III: flow and particulate dynamics during the 2003 summer coral spawning season. US Geological Survey Open-File Report 2004-1287, 36pp. http://pubs.usgs.gov/of/2004/1287/

Sun, L.C., 1996. The Maui algal bloom: the role of physics. In: Wiltse, W. (Ed.), Algal Blooms: Progress Report on Scientific Research. West Maui Watershed Management Project, pp. 54–57.

Szmant, A.M., 2002. Nutrient enrichment on coral reefs: is it a major cause of coral reef decline? Estuaries 25 (4b), 743–766.

Tartinville, B., Rancher, J., 2000. Wave-induced flow over Mururoa Atoll reef. Journal of Coastal Research 16 (3), 776–781.

Umezawa, Y., Miyajima, T., Kayanne, H., Koike, I., 2002. Significance of groundwater nitrogen discharge into coral reefs at Ishigaki Island, southwest of Japan. Coral Reefs 21, 346–356.

University of Hawaii, 2004. Department of Oceanography, Coastal wave measuring buoys program online data: http://www.soest.hawaii.edu/~buoy/

West Maui Watershed Management Project, 1996. Algal Blooms: Progress Report on Scientific Research. West Maui Watershed Algal Bloom Task Force, Maui, Hawaii 64pp.